Table 3 Parametric study involving sensors: experimental and theoretical results, ratio of closed- over open-loop rms values (%)

Frequency band, Hz	CL1		CL2		CL3	
	A2	SG3	A2	SG3	A2	SG3
			FC1			
5–25	97.1 (98.2)[a]	99.7 (99.3)	70.3 (71.7)	69.4 (75.9)	64.8 (68.2)	70.0 (74.5)
25–100	82.6 (81.6)	92.6 (87.5)	57.8 (53.0)	42.5 (42.0)	84.9 (86.2)	67.2 (72.8)
5–100	83.3 (82.3)	98.8 (97.7)	58.5 (53.9)	66.7 (72.0)	84.9 (85.5)	69.6 (74.2)
			FC3			
5–25	97.0 (97.0)	98.0 (98.9)	93.3 (93.4)	91.7 (94.0)	92.4 (95.9)	93.0 (95.0)
25–100	81.8 (79.6)	90.0 (92.2)	86.9 (86.2)	82.0 (79.9)	94.1 (95.6)	87.6 (86.5)
5–100	83.1 (81.1)	97.6 (98.5)	87.3 (86.7)	91.3 (93.3)	93.9 (95.6)	92.8 (94.5)
			FC5			
5–25	98.0 (99.5)	98.0 (99.9)	92.3 (93.4)	91.7 (94.0)	93.0 (92.5)	92.6 (96.2)
25–100	88.0 (88.7)	95.3 (94.4)	86.9 (86.2)	82.0 (79.9)	98.2 (95.1)	92.4 (88.5)
5–100	88.3 (89.1)	97.7 (99.3)	87.3 (86.7)	91.3 (93.3)	98.0 (95.0)	92.6 (95.4)

[a](Expected values).

those obtained for mode 2. The best results were obtained when the signal from SG3 was used in the feedback loop, as in case of CL2 and CL3, confirming the initial predictions. Note that CL1 was in the case of FC1 limited in gain to guarantee the controller stability.

The most severe, FC6 was the last to be tested. Because of the accumulative fatigue of the hardware (piezoelectric elements), several attempts to close the loop with the MIMO controller were unsuccessful. During each attempt, an actuator on the upper group failed, resulting in a system automatic shutdown. The apparent reason was the proximity of these actuators to the most stressed region of the fin, near the load cell. Therefore, a single input/single output (SISO) controller was designed for commanding only the lower group of actuators to reduce buffeting in the first bending mode of the tail during a closed-loop run at FC6. When feedback from accelerometer A2 and a nominal gain setting to increase chances of success were used, this SISO controller reduced the rms strain at SG3 by approximately 3% in the frequency range of 10–20 Hz. Between 0 and 100 Hz, the rms strain at SG3 was reduced by approximately 2.5%.

Conclusions

A full-scale aircraft instrumented to reduce buffet loads was tested. The test represents an important step in the development of adaptive smart structures systems. Two groups of actuators consisting of piezoelectric elements distributed over the structure were designed to achieve authority over the first and second modes of the vertical fin.

Very promising results were obtained in parametric studies using different sensors in a two input/two output controller using the standard time-invariant linear quadratic Gaussian control law design. Based on the most important performance metric, the strain gauge located at the critical point for fatigue, vertical fin buffet attenuation of 57.5% (mode 2) and 33.3% (modes 1 and 2) for the nominal FC were observed during the tests. Also, attenuation of 18.3% (mode 2) and 8.7% (modes 1 and 2) were verified for the next most severe buffeting case. In general, the CL that included at least one strain gauge in the feedback loop revealed better performance. This is an indication that strain gauges can be better correlated to the control objective, which is to reduce the structural strain generated by buffeting.

References

[1]Zimmerman, N. H., Ferman, M. A., Yurkovich, R. N., and Gerstenkorn, G., "Prediction of Tail Buffet Loads for Design Application," *Proceedings of the AIAA/ASME/ASCE/AHS/ASC 30th Structures, Structural Dynamics and Materials Conference*, AIAA, Washington, DC, 1989, pp. 1911–1919.

[2]Ferman, M. A., Patel, S. R., Zimmerman, N. H., and Gerstenkorn, G., "A Unified Approach to Buffet Response of Fighter Aircraft Empennage," *Aircraft Dynamic Loads Due to Flow Separation*, CP-483, AGARD, 1990, pp. 2.1–2.18.

[3]Lee, B. H. K., Brown, D., Zgela, M., and Poirel, D., "Wind Tunnel and Flight Tests of Tail Buffet on the CF-18 Aircraft," *Aircraft Dynamic Loads Due to Flow Separation*, CP-483, AGARD, 1990, pp. 1.1–1.26.

[4]Edwards, J. W., "Unsteady Airloads Due to Separated Flow on Airfoils and Wings," *Aircraft Dynamic Loads Due to Flow Separation*, CP-483, AGARD, 1990, pp. 16.1–16.18.

[5]Rock, S. M., Ashley, H., Digumarthi, R., and Chaney, K., "Active Control for Fin Buffet Alleviation," *Proceedings of Advances in Aerospace Sciences: A Tribute to Prof. Holt Ashley*, Stanford Univ. Press, Stanford, CA, 1993, pp. 413–421.

[6]Nitzsche, F., Zimcik, D. G., and Langille, K., "Active Control of Vertical Fin Buffeting with Aerodynamic Control Surface and Strain Actuation," *Proceedings of the AIAA/ASME/AHS Adaptive Structures Forum*, AIAA, Washington, DC, 1997, pp. 1467–1477.

[7]Moses, R. W., "Vertical Tail Buffeting Alleviation Using Piezoelectric Actuators," *Proceedings of SPIE 4th Annual International Symposium on Smart Structures and Materials, Industrial and Commercial Applications of Smart Structures Technologies*, Vol. 3044, Society of Photo-Optical Instrumentation Engineers, Bellingham, WA, 1997.

Digital Redesign of Linear State-Feedback Law via Principle of Equivalent Areas

Tohru Ieko*
Japan Defense Agency, Meguro, Tokyo 153-8630, Japan
and
Yoshimasa Ochi† and Kimio Kanai‡
National Defense Academy, Yokosuka, Kanagawa 239-8686, Japan

Introduction

DIGITAL redesign is an approach to design of a discrete-time (DT) controller via conversion of a continuous-time (CT) controller. There are some advantages of the digital redesign: First, a lot of design methods are available for CT controller design. Second, the behavior of CT systems can be physically more easily understood, which makes analysis and synthesis of CT control systems simpler without being bothered with selection of sampling periods. Third, changing the sampling period does not require total redesign of the control system, but just requires conversion of the CT controller for a new sampling period. In addition, intersampling behavior, which is sometimes overlooked in the direct DT controller design, can be taken into account. Particularly, digital redesign methods that preserve the closed-loop characteristics of the original CT control systems[1–7] are more effective for larger sampling periods than open-loop redesign methods such as Tustin's (see Ref. 8). We proposed a closed-loop digital redesign method for one-degree-of-freedom dynamic compensators[7] based on the principle of equivalent areas (PEA).[9] In this Note, we present a digital redesign method for a linear state-feedback control law also based on the PEA. That is, the DT input is determined so that the integral of the closed-loop CT

Received 14 March 2000; revision received 16 February 2001; accepted for publication 26 February 2001.

*Major, Japan Ground Self Defense Force, Technical Research and Development Institute, 2-2-1 Nakameguro.

†Associate Professor, Department of Aerospace Engineering, 1-10-20 Hashirimizu. Senior Member AIAA.

‡Professor, Department of Aerospace Engineering, 1-10-20 Hashirimizu. Associate Fellow AIAA.

input over one sampling period can be equal to that of the DT one, where the zero-order hold is utilized for hold operation. With this idea we derive DT feedback and feedforward gain matrices from the step average model[7] of the CT closed-loop system, which is a DT model that satisfies the PEA for the CT model, and mention some features of the redesigned control law. The redesign method yields exactly the same results as a different approach in Ref. 5 in the case of $N=\infty$. In Ref. 5, the CT closed-loop state euation for a piecewise-constant reference input is discretized using a Chebyshev quadrature formula to discretize the contribution of the CT feedback input. Then the DT gain matrices are determined so that the discretized state equation agrees with the state equation of the DT control system. The same results are also obtained in Ref. 6 using the improved block-pulse function. It is also found that the PEA holds in a pulse-width-modulation (PWM) control law derived from the DT or pulse-amplitude-modulation (PAM) control law, providing results with a good agreement between the PAM and PWM control systems in terms of time responses of the states.[5,10] Thus, the PEA is an attractive and effective idea in control input conversion from CT to DT as well as PAM to PWM. An application of the linear state-feedback digital redesign and PWM control methods to spacecraft motion control is shown in Ref. 11.

DT Models and PEA

Step Invariance DT Model

Consider a CT linear time-invariant (LTI) system described by

$$\dot{\boldsymbol{x}}(t)=\boldsymbol{A}\boldsymbol{x}(t)+\boldsymbol{B}\boldsymbol{u}(t), \qquad \boldsymbol{A}\in R^{n\times n}, \qquad \boldsymbol{B}\in R^{n\times r} \tag{1}$$

$$\boldsymbol{y}(t)=\boldsymbol{C}\boldsymbol{x}(t)+\boldsymbol{D}\boldsymbol{u}(t), \qquad \boldsymbol{C}\in R^{p\times n}, \qquad \boldsymbol{D}\in R^{p\times r} \tag{2}$$

where $\boldsymbol{x}(t)\in R^n$, $\boldsymbol{u}(t)\in R^r$, and $\boldsymbol{y}(t)\in R^p$ are state, input, and output vectors, respectively, and $\boldsymbol{A}$, $\boldsymbol{B}$, $\boldsymbol{C}$, and $\boldsymbol{D}$ are constant matrices. The step invariance model of the CT system for a sampling period T is defined as

$$\varepsilon\boldsymbol{x}_d(kT)=[\boldsymbol{x}_d(kT+T)-\boldsymbol{x}_d(T)]/T=\boldsymbol{A}_S\boldsymbol{x}_d(kT)+\boldsymbol{B}_S\boldsymbol{u}_d(kT) \tag{3}$$

$$\boldsymbol{y}_d(kT)=\boldsymbol{C}\boldsymbol{x}_d(kT)+\boldsymbol{D}\boldsymbol{u}_d(kT) \tag{4}$$

for a piecewise-constant input $\boldsymbol{u}(t)=\boldsymbol{u}_d(kT)$ for $kT\le t\le kT+T$, where $\boldsymbol{A}_S=(e^{AT}-\boldsymbol{I}_n)/T$,

$$\boldsymbol{B}_S=\frac{1}{T}\int_0^T e^{A\rho}\,\mathrm{d}\rho\boldsymbol{B}$$

and ε is the delta operator defined as $\varepsilon=(z-1)/T$ using the shift operator z. $\boldsymbol{I}_n$ is an $n\times n$ identity matrix. When a function $E(\boldsymbol{A},T)$ is defined as

$$E(\boldsymbol{A},T)=\sum_{n=0}^{\infty}\frac{(AT)^n}{(n+1)!}$$

$\boldsymbol{A}_S$ and $\boldsymbol{B}_S$ can be written as $\boldsymbol{A}_S=E(\boldsymbol{A},T)\boldsymbol{A}=\boldsymbol{A}E(\boldsymbol{A},T)$ and $\boldsymbol{B}_S=E(\boldsymbol{A},T)\boldsymbol{B}$, respectively.

Step Average Model[7]

The mean value $\tilde{\boldsymbol{y}}_d(kT)$ of the CT system's output over the sampling period is given by

$$\begin{aligned}\tilde{\boldsymbol{y}}_d(kT)&=\frac{1}{T}\int_0^T\boldsymbol{y}(kT+m)\,\mathrm{d}m=\boldsymbol{C}\cdot E(\boldsymbol{A},T)\boldsymbol{x}_d(kT)\\&\quad+\left\{\boldsymbol{D}+\frac{1}{T}\boldsymbol{C}\int_0^T mE(\boldsymbol{A},T)\,\mathrm{d}m\,\boldsymbol{B}\right\}\boldsymbol{u}_d(kT)\\&=\boldsymbol{C}\cdot E(\boldsymbol{A},T)\boldsymbol{x}_d(kT)+\left\{\boldsymbol{D}+\frac{1}{T}\boldsymbol{C}\boldsymbol{A}^{-2}\left(e^{AT}-\boldsymbol{I}_n\right.\right.\\&\quad\left.\left.-\boldsymbol{A}T\right)\boldsymbol{B}\right\}\boldsymbol{u}_d(kT):=\tilde{\boldsymbol{C}}\boldsymbol{x}_d(kT)+\tilde{\boldsymbol{D}}\boldsymbol{u}_d(kT)\end{aligned} \tag{5}$$

Note that the state equation of this model is the same as that of the step invariance model described by Eq. (3). Let us call the DT model described by Eqs. (3) and (5) the step average model.

PEA

Consider a DT input $\boldsymbol{u}_d(kT)$ associated with a CT control input $\boldsymbol{u}(t)$ that satisfies the following equation:

$$\boldsymbol{u}_d(kT)=\frac{1}{T}\int_{kT}^{kT+T}\boldsymbol{u}(t)\,\mathrm{d}t \tag{6}$$

Equation (6) defines the PEA. It is shown using the mean value theorem that the DT control input reproduces time responses of the states to the CT control input with a good precision; that is, the difference between the CT and DT states at $t=kT+T$ is of the order of T^2 (Ref. 7).

Digital Redesign Based on PEA

In open-loop digital redesign methods such as Tustin's, a very fast sampling rate is often required to guarantee stability and good control performance. However, digital redesign methods that allow a larger sampling period are desired to relax a high-performance requirement for onboard computers. As already mentioned, generally closed-loop redesign methods are superior to open-loop ones for larger sampling periods in stability and performance. The proposed method is of the closed-loop type.

Suppose that for a CT plant described by Eqs. (1) and (2) a CT state-feedback control law

$$\boldsymbol{u}(t)=\boldsymbol{F}\boldsymbol{x}(t)+\boldsymbol{G}\boldsymbol{r}(t) \tag{7}$$

is given, where $\boldsymbol{F}$ and $\boldsymbol{G}$ are constant matrices and $\boldsymbol{r}(t)$ is a piecewise-constant external input, that is, $\boldsymbol{r}(t)=\boldsymbol{r}_d(kT)$ for $kT\le t\le kT+T$. The CT plant-input transfer function $\boldsymbol{H}(s)$, which is a closed-loop transfer function from the external input $\boldsymbol{r}(t)$ to the control input of the plant $\boldsymbol{u}(t)$, can be written as

$$\boldsymbol{H}(s)=\boldsymbol{F}(s\boldsymbol{I}_n-\boldsymbol{A}-\boldsymbol{B}\boldsymbol{F})^{-1}\boldsymbol{B}\boldsymbol{G}+\boldsymbol{G} \tag{8}$$

Let us assume that the zero-order hold is used in application of DT plant-input $\boldsymbol{u}_d(kT)$. If the DT input $\boldsymbol{u}_d(kT)$ is determined to satisfy Eq. (6) for the CT control input of Eq. (7) in the feedback form or Eq. (8) in the closed-loop form, then by replacing $\boldsymbol{A}$, $\boldsymbol{B}$, $\boldsymbol{C}$, and $\boldsymbol{D}$ in Eq. (5) by $\boldsymbol{A}+\boldsymbol{B}\boldsymbol{F}$, $\boldsymbol{B}\boldsymbol{G}$, $\boldsymbol{F}$, and $\boldsymbol{G}$, respectively, the DT control law is given by

$$\boldsymbol{u}_d(kT)=\boldsymbol{F}_d\boldsymbol{x}_d(kT)+\boldsymbol{G}_d\boldsymbol{r}_d(kT) \tag{9}$$

where, defining $\boldsymbol{A}_c=\boldsymbol{A}+\boldsymbol{B}\boldsymbol{F}$,

$$\boldsymbol{F}_d=\boldsymbol{F}E(\boldsymbol{A}_c,T) \tag{10}$$

$$\begin{aligned}\boldsymbol{G}_d&=\boldsymbol{G}+(1/T)\boldsymbol{F}\boldsymbol{A}_c^{-2}\left(e^{A_cT}-\boldsymbol{I}_n-\boldsymbol{A}_cT\right)\boldsymbol{B}\boldsymbol{G}\\&=\left\{\boldsymbol{I}_r+\boldsymbol{F}\boldsymbol{A}_c^{-1}[E(\boldsymbol{A}_c,T)-\boldsymbol{I}_n]\boldsymbol{B}\right\}\boldsymbol{G}\end{aligned} \tag{11}$$

The gain matrices $\boldsymbol{F}_d$ and $\boldsymbol{G}_d$ are exactly the same as $\boldsymbol{K}_{dr}$ and $\boldsymbol{E}_{dr}$ for $N=\infty$ in Ref. 5 and $\boldsymbol{K}_d$ and $\boldsymbol{E}_d$ in Ref. 6, respectively. The derivation of the redesigned gain matrices in Ref. 6 is also based on Eq. (6). However, we insist that Eq. (6) or he PEA be a general rule for digital redesign and that the DT system that satisfies the PEA be described as a step average model.

This digital redesign method has the following features:

1) As $T\to 0$, the obtained gains become the original CT ones.

2) Although the redesigned closed-loop system matrix $\boldsymbol{A}_S+\boldsymbol{B}_S\boldsymbol{F}_d$ is different from the desired one $(\boldsymbol{e}^{A_cT}-\boldsymbol{I}_n)/T$, the first-order approximation of the sampling period is achieved in the delta form. In fact, from the Taylor series expansion around $T=0$, it follows that

$$\left(\boldsymbol{e}^{A_cT}-\boldsymbol{I}_n\right)/T-(\boldsymbol{A}_S+\boldsymbol{B}_S\boldsymbol{F}_d)=-\boldsymbol{A}\boldsymbol{B}\boldsymbol{F}\boldsymbol{A}_cT^2/12+\boldsymbol{R}(T^3) \tag{12}$$

where $\boldsymbol{R}(T^3)$ denotes the error of the order of T^3. This feature provides stability for relatively large sampling periods.

3) If the redesigned digital control system is stable, then DT steady states are equivalent to CT steady states, that is,

$$\begin{aligned}\boldsymbol{x}_d(\infty)&=-(\boldsymbol{A}_S+\boldsymbol{B}_S\boldsymbol{F}_d)^{-1}\boldsymbol{B}_S\boldsymbol{G}_d\\&=-(\boldsymbol{E}_o\boldsymbol{A}+\boldsymbol{E}_o\boldsymbol{B}\boldsymbol{F}\boldsymbol{E}_c)^{-1}\boldsymbol{E}_o\boldsymbol{B}\left\{\boldsymbol{I}_r+\boldsymbol{F}\boldsymbol{A}_c^{-1}(\boldsymbol{E}_c-I_n)\boldsymbol{B}\right\}\boldsymbol{G}\\&=-(\boldsymbol{A}+\boldsymbol{B}\boldsymbol{F}\boldsymbol{E}_c)^{-1}\{\boldsymbol{A}_c+\boldsymbol{B}\boldsymbol{F}(\boldsymbol{E}_c-\boldsymbol{I}_n)\}\boldsymbol{A}_c^{-1}\boldsymbol{B}\boldsymbol{G}\\&=-\boldsymbol{A}_c^{-1}\boldsymbol{B}\boldsymbol{G}=\boldsymbol{x}(\infty)\end{aligned} \tag{13}$$

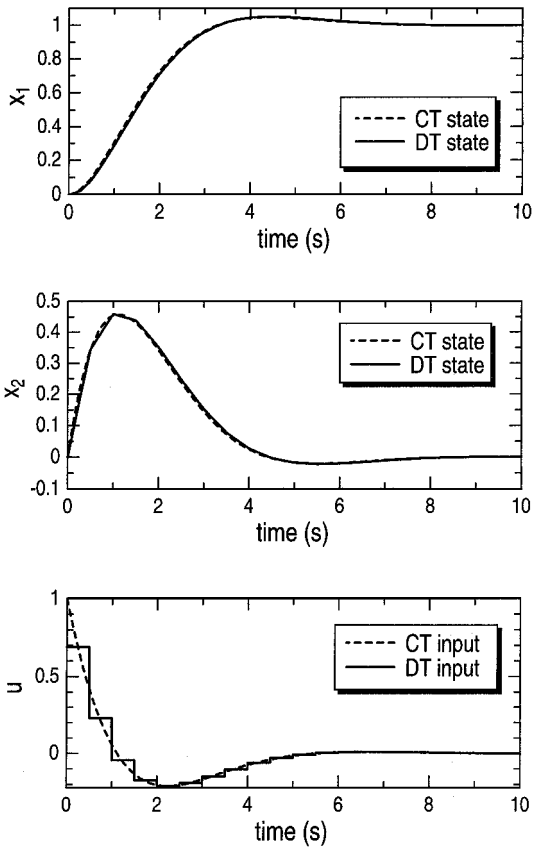

Fig. 1 Time histories of states and inputs.

where $\boldsymbol{E}_o = E(\boldsymbol{A}, T)$ and $\boldsymbol{E}_c = E(\boldsymbol{A}_c, T)$.

Numerical Example

The effectiveness of the redesigned control law is illustrated by a simple numerical example. Let us consider a CT-LTI system described by Eq. (1) with

$$\boldsymbol{A} = \begin{bmatrix} 0 & 1 \\ 0 & 0 \end{bmatrix}, \qquad \boldsymbol{B} = \begin{bmatrix} 0 \\ 1 \end{bmatrix} \tag{14}$$

The feedback gain matrix $\boldsymbol{F} = [-1 \quad -1.4]$ gives the closed-loop system a second-order dynamics with a damping ratio 0.7 and a natural frequency 1 rad/s. For a sampling time $T = 0.5$ s and the feedforward gain matrix $\boldsymbol{G} = 1$, the DT gain matrices are computed by Eqs. (10) and (11) as

$$\boldsymbol{F}_d = -[0.6898 \quad 0.1624], \qquad \boldsymbol{G}_d = 0.6898 \tag{15}$$

Figure 1 shows time histories of the states and control input of the CT and DT closed-loop systems for a step input $r(t) = 1$. The DT state responses agree with the CT ones very well, and it can be seen that the DT control input satisfies the PEA in each sampling period.

Conclusions

A digital redesign method for the linear state-feedback control law is derived based on the PEA. The effectiveness of the DT control law is illustrated through a numerical example. The redesigned control law is the same as the one derived by other approaches. As mentioned in the Introduction, however, the PEA also plays an important role in redesign of one-degree-of-freedom controllers and conversion of PAM inputs into PWN inputs. These characteristics of the PEA imply that the PEA is an underlying idea generally applicable to control-input redesign, and the analysis using the mean value theorem explains why it does work.

References

[1] Kuo, B. C., and Peterson, D. W., "Optimal Discretization of Continuous-Data Control Systems," *Automatica*, Vol. 9, No. 1, 1973, pp. 125–129.

[2] Rattan, K. S., "Digitalization of Existing Continuous Control Systems," *IEEE Transactions on Automatic Control*, Vol. 29, No. 3, 1984, pp. 282–285.

[3] Keller, J. P., and Anderson, B. D. O., "A New Approach to the Discretization of Continuous-Time Controllers," *IEEE Transactions on Automatic Control*, Vol. 37, No. 2, 1992, pp. 214–223.

[4] Markazi, A. H. D., and Hori, N., "A New Method with Guaranteed Stability for Discretization of Continuous-Time Control Systems," *Proceedings of American Control Conference*, Vol. 2, Omnipress, Madison, WI, 1992, pp. 1397–1402.

[5] Shieh, L.-S., Wang, W.-M., and Sunkel, J. W., "Design of PAM and PWM Controllers for Sampled-Data Interval Systems," *Journal of Dynamic Systems, Measurement, and Control*, Vol. 118, Dec. 1996, pp. 673–682.

[6] Tsai, J. S. H., Shieh, L. S., and Zhang, J. L., "An Improvement of the Digital Redesign Method Based on the Block-Pulse Function Approximation," *Circuits, Systems and Signal Processing*, Vol. 12, No. 1, 1993, pp. 37–49.

[7] Ieko, T., Ochi, Y., and Kanai, K., "New Design Method for Pulse-Width Modulation Control System via Digital Redesign," *Journal of Guidance, Control, and Dynamics*, Vol. 22, No. 1, 1999, pp. 461–467.

[8] Franklin, G. F., Powell, J. D., and Workman, M. L., "Design of Discrete Equivalents by Numerical Integration," *Digital Control of Dynamic Systems*, 2nd ed., Addison Wesley Longman, Reading, MA, 1990, pp. 135–147.

[9] Andeen, R. E., "The Principle of Equivalent Areas," *Proceedings of the American Institute of Electrical Engineers Pacific General Meeting*, Vol. 79, American Inst. of Electrical Engineers, Applications and Industry, Nov. 1960, pp. 332–336.

[10] Bernelli-Zazzera, F., Mantegazza, P., and Nurzia, V., "Multi-Pulse-Width Modulated Control of Linear Systems," *Journal of Guidance, Control, and Dynamics*, Vol. 21, No. 1, 1998, pp. 64–70.

[11] Ieko, T., Ochi, Y., and Kanai, K., "Design of a Pulse-Width-Modulation Spacecraft Attitude Control System via Digital Redesign," *Proceedings of the 14th IFAC World Congress*, Vol. P, Pergamon, Oxford, England, U.K., 1999, pp. 355–360.

Variable Structure Controller Design with Application to Missile Tracking

M. Seetharama Bhat,* D. Sasi Bai,† A. A. Powly,‡
K. N. Swamy,§ and D. Ghose*
Indian Institute of Science, Bangalore 560 012, India

Introduction

THIS Note presents the robust autopilot design for missile tracking problem employing variable structure control (VSC) with a power rate reaching law. VSC systems (VSCS) have been extensively studied in the literature over the past 40 years.[1–3] VSC with sliding mode (SM) is a robust nonlinear control for controlling uncertain plants. Robustness is the most important virtue of VSCS. A VSC is characterized by a discontinuous feedback control structure that is switched as the system state crosses certain user specified surfaces called switching surfaces (SS) or sliding surfaces. The control strategy is selected to steer the system state trajectory from any initial state onto the SS and thereafter to constrain the state trajectory motion in the close vicinity of the SS. This results in a reduced-order, surface-dependent sliding motion that is insensitive to disturbance and parameter variations. Assuming all states are available, a linear SS $\sigma[x(t)]$ is used in the present work. Chattering is an undesirable feature of VSC, and it can be eliminated by the continuation method or by the reaching law method.[4]

Missile autopilots are designed to improve stability and performance. The dynamics of the missile are nonlinear, time varying, and coupled.[5] Thukral and Innocenti present VSC design for a missile autopilot that uses both aerodynamic control and reaction jet

Received 13 April 2000; revision received 18 December 2000; accepted for publication 5 January 2001.

*Professor, Department of Aerospace Engineering.
†Project Associate, Department of Aerospace Engineering.
‡Research Scholar, Department of Aerospace Engineering.
§Deceased, Joint Advance Technology Program.